Triggering of Microseismicity During Low Tides at the Equatorial Mid-Atlantic Ridge, Inferred from the PI-LAB Experiment Data

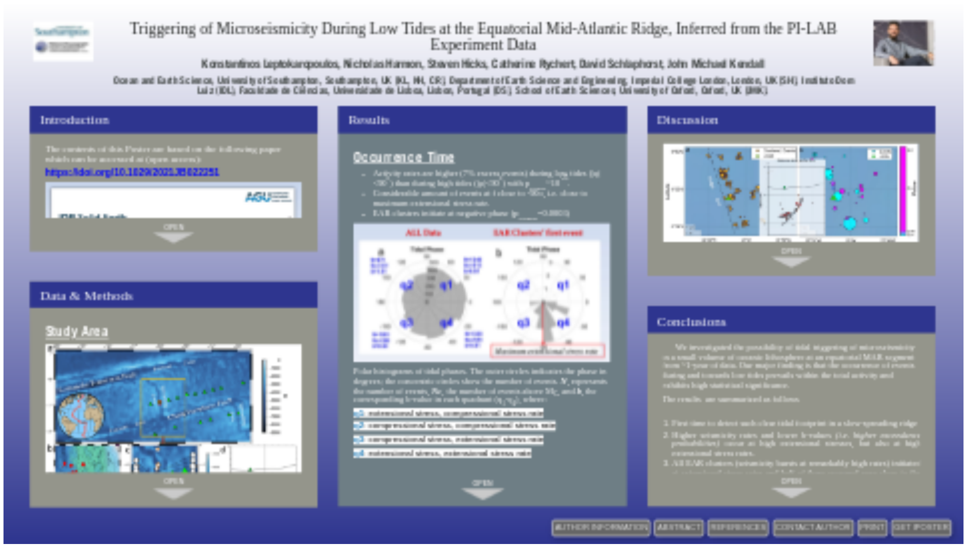

Konstantinos Leptokaropoulos, Nicholas Harmon, Steven Hicks, Catherine Rychert, David Schlaphorst, John Michael Kendall

Ocean and Earth Science, University of Southampton, Southampton, UK [KL, NH, CR], Department of Earth Science and Engineering, Imperial College London, London, UK [SH], Instituto Dom Luiz (IDL), Faculdade de Ciências, Universidade de Lisboa, Lisbon, Portugal [DS], School of Earth Sciences, University of Oxford, Oxford, UK [JMK].

PRESENTED AT:

INTRODUCTION

Click **here (http://agu2021fallmeeting-agu.ipostersessions.com/Default.aspx?s=02-94-12-D0-C2-9D-A4-11-A1-E9-01-69-06-45-81-0F)** for Interactive poster version

The contents of this Poster are based on the following paper which is available at (open access):

https://doi.org/10.1029/2021JB022251 (https://doi.org/10.1029/2021JB022251)

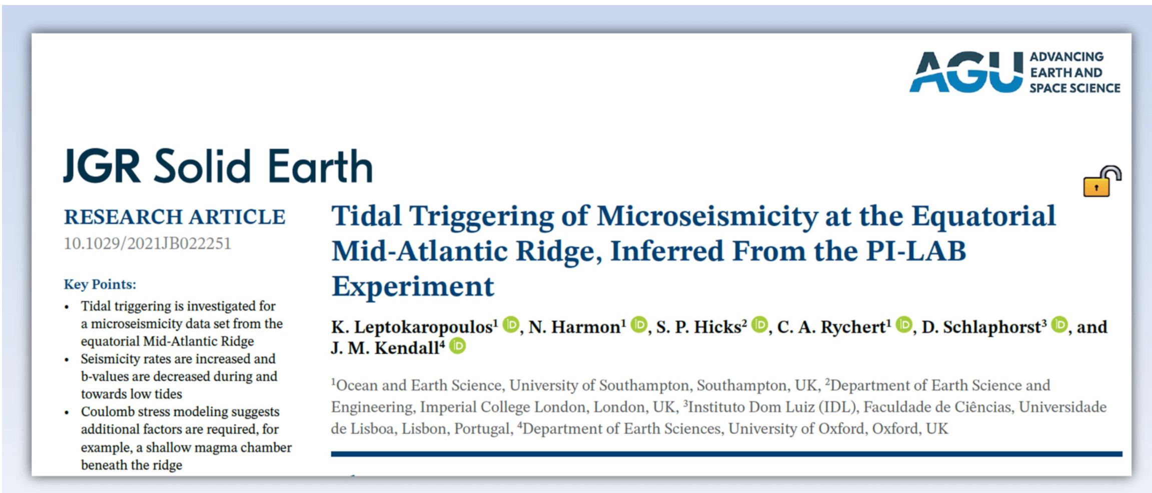

ADVANCING EARTH AND SPACE SCIENCE

JGR Solid Earth

RESEARCH ARTICLE
10.1029/2021JB022251

Key Points:
- Tidal triggering is investigated for a microseismicity data set from the equatorial Mid-Atlantic Ridge
- Seismicity rates are increased and b-values are decreased during and towards low tides
- Coulomb stress modeling suggests additional factors are required, for example, a shallow magma chamber beneath the ridge

Tidal Triggering of Microseismicity at the Equatorial Mid-Atlantic Ridge, Inferred From the PI-LAB Experiment

K. Leptokaropoulos[1], N. Harmon[1], S. P. Hicks[2], C. A. Rychert[1], D. Schlaphorst[3], and J. M. Kendall[4]

[1]Ocean and Earth Science, University of Southampton, Southampton, UK, [2]Department of Earth Science and Engineering, Imperial College London, London, UK, [3]Instituto Dom Luiz (IDL), Faculdade de Ciências, Universidade de Lisboa, Lisbon, Portugal, [4]Department of Earth Sciences, University of Oxford, Oxford, UK

We use the seismicity data acquired by the PI-LAB and EURO-LAB projects to investigate the role of tides as a triggering mechanism of microseismicity along a segment of the equatorial MAR. We study the correlation between ocean tide phase and amplitude with the occurrence of seismicity. Then, we identify seismic sequences characterised by enhanced activity rates (i.e. temporal clusters) separated by time periods in which seismic activity falls well below the reference seismicity level. We also demonstrate how the magnitude distribution of seismicity is influenced by tidal fluctuations. Finally, we interpret the results in terms of Coulomb stress changes and extract information on frictional and hydraulic properties of the lithosphere in the close vicinity of the axial ridge.

DATA & METHODS

Study Area

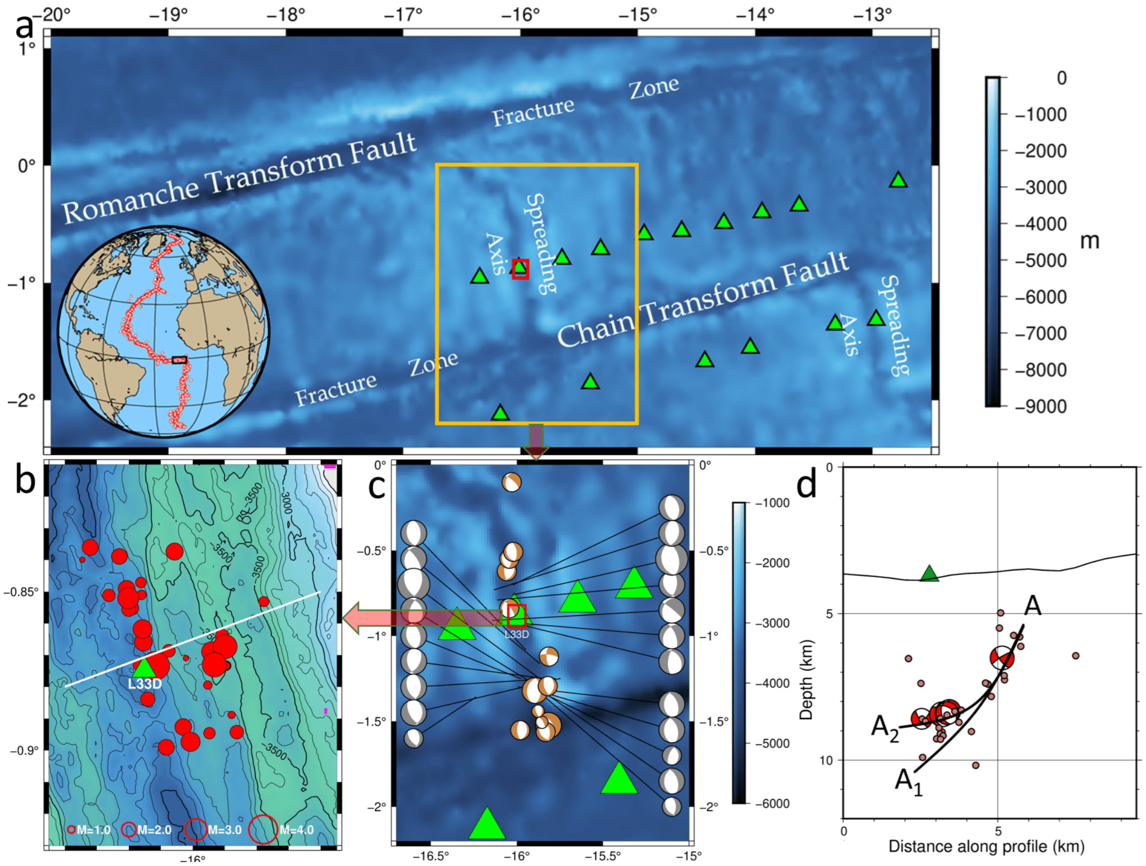

(a) Regional map of equatorial Atlantic. Green triangles denote the location of OBS stations operated during the PI-LAB experiment.

(b) Bathymetric map of the study area. Red circles indicate the 34 seismicity templates used to compile our catalogue.

(c) Broader area focused on the ridge spreading axis shown in (a). Focal mechanisms are from GCMT (Ekström et al., 2012; grey) and this study (brown).

(d) Double difference locations of the 34 template events and available focal mechanisms, projected along the cross-section shown in (b), suggest possible reactivations of a west-dipping normal fault.

Seismicity Data

1-year seismicity data (March 2016 - March 2017)

- ❑ Detection and Location: Lassie (Heimann et al., 2017)
- ❑ Relocation: NonLinLoc (Lomax et al., 2000) and DD (Waldhauser and Elsworth, 2000)

↓

- ❑ 34 well-located events,~5km from L33D station, mean vertical error ~200m.

↓

- ❑ Used as templates within EQcorrscan (Chamberlain et al., 2018).

↓

4719 events, with -1.4≤M_L≤ 4.0 ➡ **1781 events above M_C=0.0**

(single station estimates, unknown M_L-M_W scaling)

- We define as **Enhanced Activity Rate (EAR)** Clusters, sequences with >10 events and maximum interevent time between subsequent events <30 min. 14 such EAR clusters (301 events) were identified, having 25-200 times higher rates than the overall seismic activity.

Methods

- The SPOTL software (Agnew, 1997) is used to calculate solid Earth tides as well as ocean loading with the global ocean tide model TPXO72.2010 (Egbert & Erofeeva, 2002).
- We define the tidal phase (see figure on the right), ***ϕ=0***, at low tides and apply the Schuster (1897) test, to quantify the randomness of seismic events' occurrence time distribution.
- We calculate tidal Coulomb stress changes (ΔCFF) considering different fault plane geometries and frictional properties.
- The completeness magnitude, M_C, is estimated by the Anderson-Darling (AD) test (Marsaglia and Marsaglia, 2004; Leptokaropoulos, 2020).

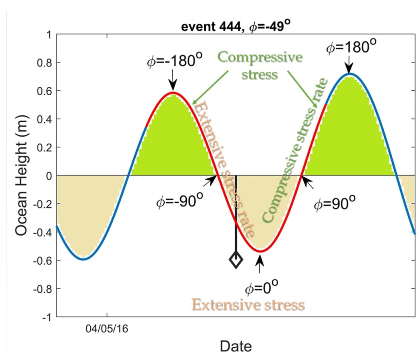

- The Maximum likelihood estimation of b-value is applied (Aki, 1965) and the significance of the b-value difference between 2 datasets is evaluated by the Akaike Information Criterion (AIC, Utsu, 1999).
- The SHAPE software (Leptokaropoulos and Lasocki, 2020) is used to calculate the exceedance probabilities for specified magnitudes and time periods.

RESULTS

Occurrence Time

- Activity rates are significantly higher (7% excess events) at low tides ($|\varphi|<90^{o}$) than at high tides ($|\varphi|>90^{o}$) with $p_{Schuster}\sim10^{-25}$.
- Considerable amount of events occur at φ close to -90^{o}, i.e. close to maximum extensional stress rate.
- EAR clusters initiate at negative phase ($p_{Schuster}=0.0003$)

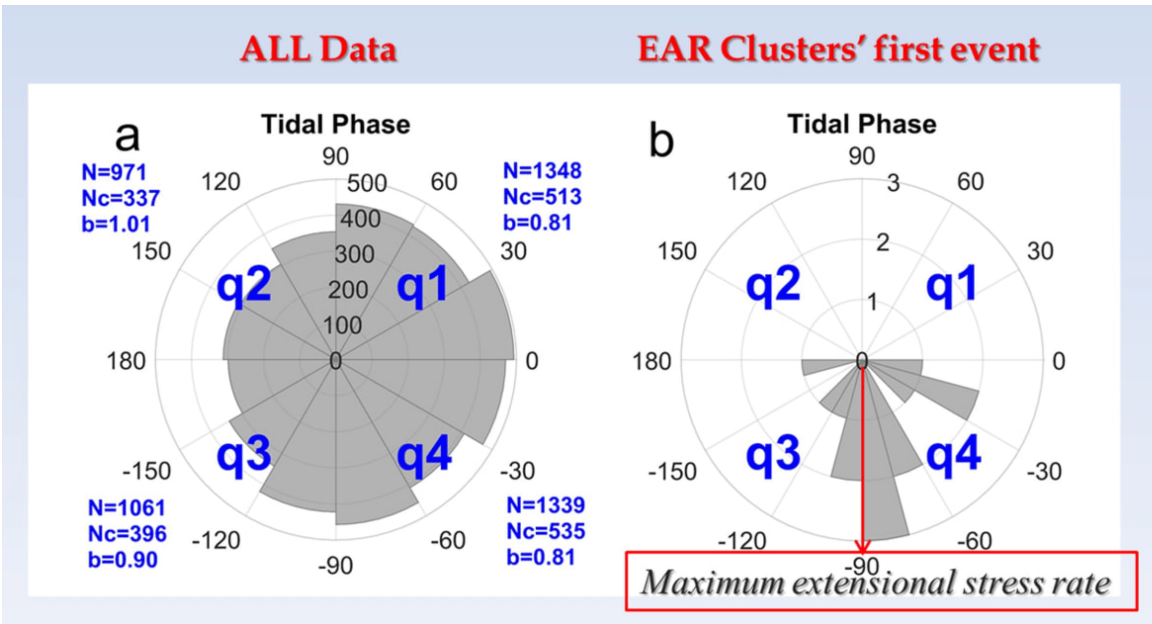

Polar histograms of tidal phases. The outer circles indicate the phase in degrees; the concentric circles show the event counts. ***N***, represents the number of events, ***Nc***, the number of events above M_C, and ***b***, the corresponding b-value in each quadrant (q_1-q_4), where:

q1: extensional stress, compressional stress rate

q2: compressional stress, compressional stress rate

q3: compressional stress, extensional stress rate

q4: extensional stress, extensional stress rate

Magnitude Distribution

- b-values exhibit significant fluctuations at high tides whereas they are far more stable at low tides
- EAR clusters have a total duration of ~1day, they accommodate 83% of the total seismic moment release of the 1-year experiment.
- Exceedance probabilities are higher during low tides, however the difference is not significant at 0.05 level.
- The 301 EAR Clustered events have $b=0.61\mp0.04$.
- The remaining 1480 (unclustered) events have $b=0.89\mp0.02$

These two b-values differ significantly (p_{AIC}~10^{-7})

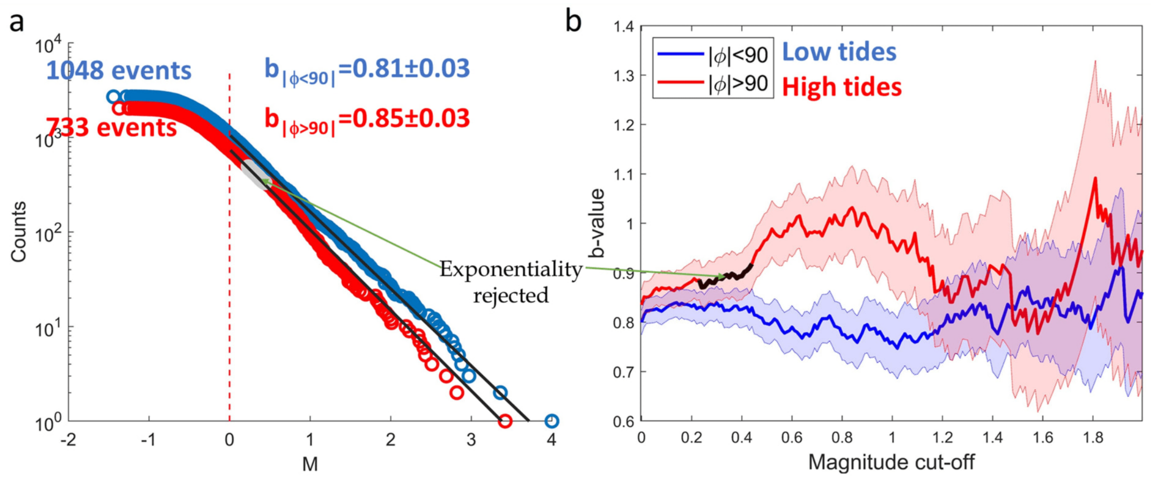

(a) Magnitude-frequency distribution with vertical dashed line indicates the M_C=0.0. (b) b-value fluctuation as a function of magnitude cut-off. The blue and red shaded areas indicate the b-value standard error. The grey segment in (a) and black segment in (b) show the range of magnitude for which the AD test rejects the null hypothesis of exponential magnitude distribution.

Coulomb Stress Calculations

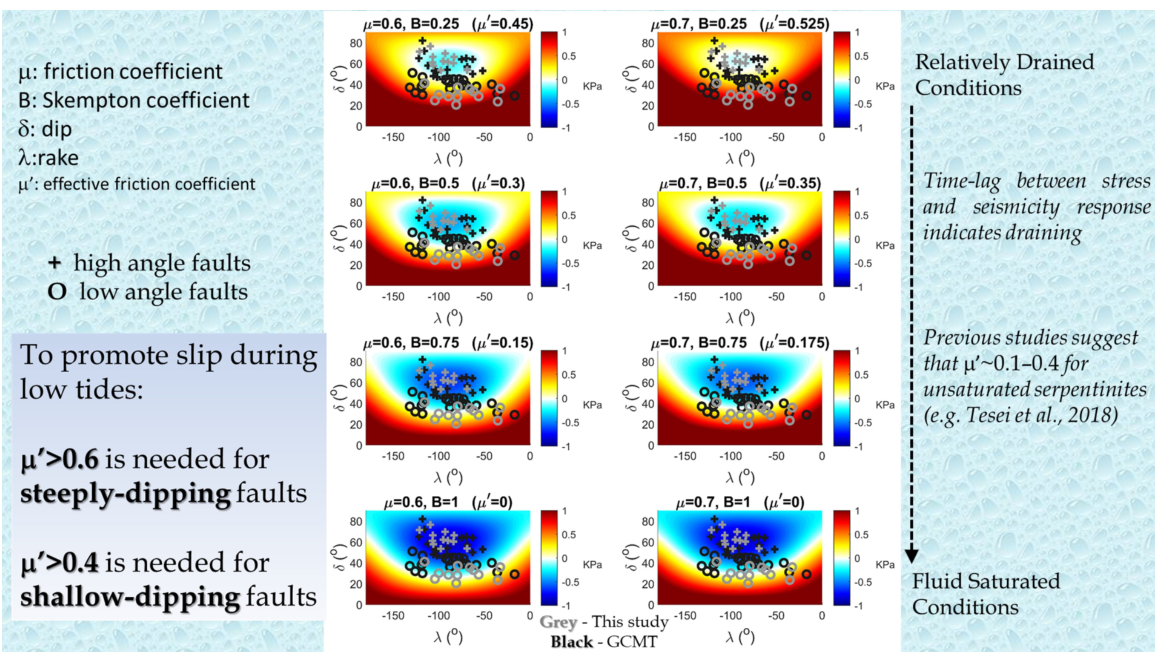

DISCUSSION

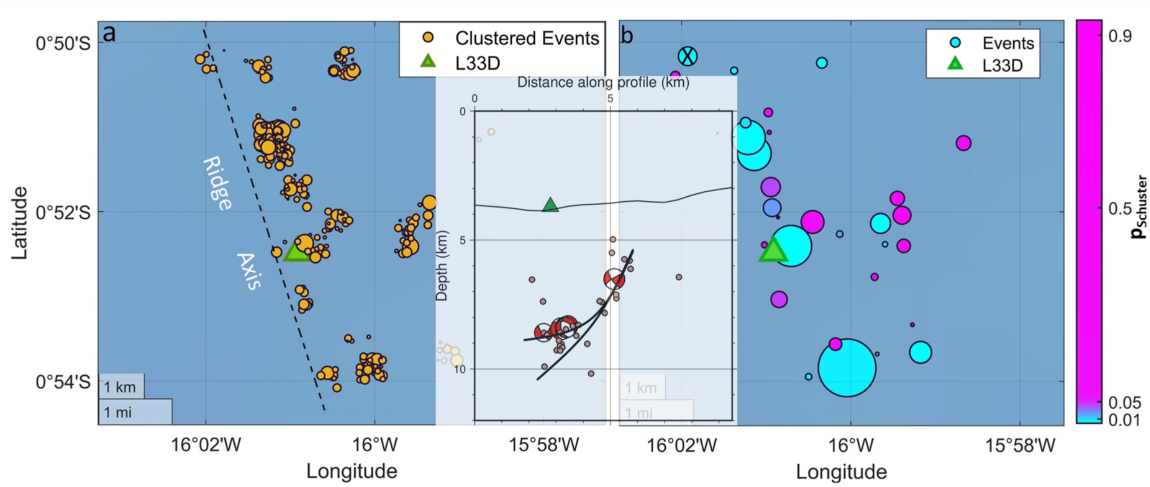

EAR clustering and tidal signal (Schuster test p-value) is stronger along the ridge axis

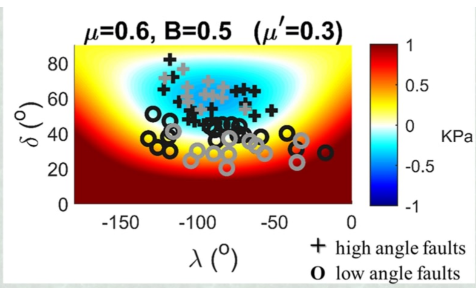

ΔCFS
- **Low angle faults (low friction)**
- **High angle faults high friction**
  - **fully drained conditions (B<0.25)**
  - **strong lithosphere**

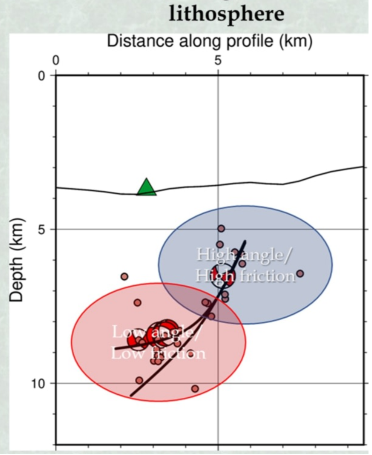

- Geological evidence support a rather weak (low friction) oceanic crust/mantle, given the abundant presence of lizardite and chrysolite serpentinites in the mantle
- Even a small degree of serpentinization (<15%) can reduce the oceanic strength to that of pure oceanic serpentinite
- The lower part of the listric fault may end in weak, serpentinized mantle
- The upper fault part may be located in the stronger, basaltic oceanic crust.

- A magma chamber could inflate owing to its higher compressibility, potentially resulting in a favourable stress field during low tides (e.g. Scholz et al., 2019). The existence of a magma chamber is supported by previous seismic imaging in the region (Saikia et al., 2021).

CONCLUSIONS

We investigated the possibility of tidal triggering of microseismicity in a small volume of oceanic lithosphere at an equatorial MAR segment from ~1-year of data. Our major finding is that the occurrence of events during and towards low tides prevails within the total activity and exhibits high statistical significance.

The results are summarized as follows

1. First time to detect such clear tidal footprint in a slow-spreading ridge
2. Higher seismicity rates and lower b-values *(i.e. higher exceedance probabilities)* occur at high extensional stresses, but also at high extensional stress rates.
3. All EAR clusters (seismicity bursts at remarkably high rates) initiated at extensional stress rates and half of them occurred very close to the maximum extensional stress rate.
4. Coulomb stress modeling is consistent with tidal triggering on low-angle normal faulting in a serpentinized, low-friction oceanic lithosphere.
5. Coulomb stress modeling suggests additional factors, such as the influence of an underlying magma chamber, are required to explain tidal triggering on high angle faults, at low tides

AUTHOR INFORMATION

Dr Konstantinos (Kostas) Leptokaropoulos (https://www.southampton.ac.uk/oes/about/staff/kl2c20.page) is a Research Fellow in Seismology at the University of Southampton (National Oceanography Centre), UK.

For more information please visit my Research Gate webpage:

https://www.researchgate.net/profile/Konstantinos-Leptokaropoulos-2
(https://www.researchgate.net/profile/Konstantinos-Leptokaropoulos-2)

and my Linkedin webpage:

https://www.linkedin.com/in/konstantinos-leptokaropoulos-391a0665/
(https://www.linkedin.com/in/konstantinos-leptokaropoulos-391a0665/)

email:K.Leptokaropoulos@soton.ac.uk

ABSTRACT

The combined gravitational pulls from the moon and the sun result in periodical tidal stresses at rates potentially exceeding the tectonic ones. Yet, tidal triggering of earthquakes in critically stressed faults is still under debate and controversial results have been obtained, depending upon specific physical properties and geological settings. Although no universal triggering pattern between earthquakes and tides has been observed in oceanic environments, previous research implies relation between increased seismicity rates and low tides at particular sites at fast-spreading ridges in the Pacific.

We present a dataset of 4719 microearthquakes ($-1.4 \leq M_L \leq 4.0$) recorded by an Ocean Bottom Seismometer (OBS) network at the slow-spreading equatorial Mid-Atlantic Ridge from March 2016 to February 2017. We use a single-station template matching technique to focus on a small volume, spreading within a ~5km radius from the station. The origin time of the events and their epicentral location is sufficiently determined for a robust comparison with the ocean tides. Our analysis suggests a significant correlation between seismic potential and tidal forces, with the majority of events occurring during or towards low tides, i.e., during maximized extensional stress and maximized extensional stress rate. The tidal dependence of magnitude distribution is also investigated. Although the b-values are generally lower at low tides, the differences are not sufficiently large to achieve statistical significance. However, seismic bursts (enhanced activity rate clusters), occurring at rates above the reference seismicity, are exclusively initiated at extensional stress rates. Coulomb stress modelling implies that slip is promoted during low tides at low-angle normal faults. Local morphology, seismicity distribution and focal mechanisms suggest the existence of high angle faults at shallower depths. Coulomb modelling suggests slip on these faults should not be triggered at low tides unless another factor is considered. One possibility is the presence of a shallow magma chamber. Such a chamber has also been suggested by previous seismic imaging results. Overall, the result yields new insight into magmatic – tectonic cycles and seismicity triggering at mid-ocean ridges.

REFERENCES

Aki, K. (1965), Maximum likelihood estimate of b in the formula logN = a − bM and its confidence limits. *Bulletin of Earthquake Research Institute of the University of Tokyo*, 43, 237–239

Agius, M. R., Harmon, N., Rychert, C. A., Tharimena, S., & Kendall, J. M. M. (2018), Sediment characterization at the equatorial Mid-Atlantic Ridge from P-to-S teleseismic phase conversions recorded on the PI-LAB experiment. *Geophysical Research Letters*, 45, 12,244–12,252, doi: 10.1029/2018GL080565 (https://doi.org/10.1029/2018GL080565)

Agius, M. R., Rychert, C. A., Harmon, N., Tharimena, S., & Kendall, J. M. (2021), A thin mantle transition zone beneath the equatorial Mid-Atlantic Ridge. *Nature*, 589, 562–566, doi: 10.1038/s41586-020-03139-x

Agnew, D. C. (1997), NLOADF: a program for computing ocean-tide loading. *Journal of Geophysical Research*, 102, 5109–5110

Bakun W. H. & Joyner W. B. (1984), The ML scale in central California. *Bulletin of the Seismological Society of America*, 74, no. 5, 1827–1843

Barreyre, T., Escartín, J., Sohn, R. A., Cannat, M., Ballu, V., & Crawford, W. C. (2014), Temporal variability and tidal modulation of hydrothermal exit-fluid temperatures at the Lucky Strike deepsea vent field, Mid-Atlantic Ridge. *Journal of Geophysical Research: Solid Earth*, 119, 2543–2566, doi:10.1002/2013JB010478

Behn, M. D., Boettcher, M. S., & Hirth, G. (2007), Thermal structure of oceanic transform faults. *Geology*, 35, 4, 307-310, doi: 10.1130/G23112A.1

Bhatnagar, T., Tolstoy, M., & Waldhauser, F. (2015), Influence of fortnightly tides on earthquake triggering at the East Pacific Rise at 9°50′N. *Journal of Geophysical Research: Solid Earth*, 121, 1262–1279, doi:10.1002/2015JB012388

Bogiatzis, P., Karamitrou, A., Ward Neale J., Harmon, N., Rychert, C. A., & Srokosz, M. (2020), Source regions of infragravity waves recorded at the bottom of the equatorial Atlantic Ocean, using OBS of the PI-LAB experiment. *Journal of Geophysical Research: Oceans*, 125, e2019JC015430

Bown, J. W. & White, R. S. (1994), Variation with spreading rate of oceanic crustal thickness and geochemistry. *Earth and Planetary Science Letters*, 121, 3-4, 435-449, doi:10.1016/0012-821X(94)90082-5 (https://doi.org/10.1016/0012-821X(94)90082-5)

Cann, J. R., Blackman, D. K., Smith, D. K., McAllister, E., Janssen, B., Mello, S., Avgerinos, E., Pascoe A. R. & Escartın, J. (1997), Corrugated slip surfaces formed at North Atlantic ridge-transform intersections. *Nature*, 385, 329–332

Chamberlain, C. J., Hopp, C. J., Boese, C. M., Warren-Smith, E., Chambers, D., Chu, S. X., Michailos, K., & Townend, J. (2018), EQcorrscan: Repeating and near-repeating earthquake detection and analysis in Python. *Seismological Research Letters*, 89, 173–181

Chatelain, J. O., Roecker, S. W., Hatzfeld, D., & Molnar, P. (1980), Microearthquake seismicity and fault plane solutions in the Hindu Kush region and their tectonic implications. *Journal of Geophysical Research*, 85, 1365-1387

Cochran, E. S., Vidale J. E., & Tanaka S. (2004), Earth tides can trigger shallow thrust fault earthquakes. *Science*, 306, 1164–1166

Christeson, G. L., Goff, J. A., & Reece, R. S. (2019), Synthesis of oceanic crustal structure from two-dimensional seismic profiles. *Reviews of Geophysics*, 57, 504–529. https://doi.org/10.1029/2019RG000641

Dunn, R. A., Arai, R., Eason, D. E., Canales, J. P., & Sohn, R. A. (2017), Threedimensional seismic structure of the mid-Atlantic ridge: An investigation of tectonic, magmatic, and hydrothermal processes in the rainbow area. *Journal of Geophysical Research: Solid Earth*, 122, 9580–9602. https://doi.org/10.1002/ 2017JB015051

Egbert, G. D. & Erofeeva, S. Y. (2002), Efficient inverse modeling of barotropic ocean tides. *Journal of Atmospheric and*

Oceanic Technology, 19, 183-204

Ekström, G, Nettles M., & Dziewoński A. M. (2012), The global CMT project 2004-2010: Centroid-moment tensors for 13,017 earthquakes. *Physics of the Earth and Planetary Interiors*, 200-201, 1-9, doi: 10.1016/j.pepi.2012.04.002 (https://doi.org/10.1016/j.pepi.2012.04.002)

El-Isa, Z. H., & Eaton, D. W. (2014), Spatiotemporal variations in the b-value of earthquake magnitude–frequency distributions: Classification and causes. *Tectonophysics*, 615-616, 1-11, doi: 10.1016/j.tecto.2013.12.001

Engeln, J. F., Weins, D. A., & Stein, S. (1986), Mechanisms and depths of Atlantic transform earthquakes. *Journal of Geophysical Research*, 91, 548–577

Escartin, J., Hirth, G., & Evans, B. (1997), Nondilatant brittle deformation of serpentinites: Implications for Mohr-Coulomb theory and the strength of faults. *Journal of Geophysical Research*, 102, 2897–2913

Escartin, J., Hirth, G., and Evans, B. (2001), Strength of slightly serpentinized peridotites: Implications for the tectonics of oceanic lithosphere. *Geology*, 29, 1023-1026

Fang, W. W., Langseth, M. G. & Schultheiss, P. J. (1993), Analysis and application of in situ pore pressure measurements in marine sediments, *Journal of Geophysical Research*, 98(B5), 7921-7938

Früh-Green, G. L., Plas, A., & Lécuyer, C. (1996), *14. Petrologic and stable isotope constraints on hydrothermal alteration and serpentinization of the EPR shallow mantle at Hess deep (site 895)*. Proceeding of the Ocean Drilling Program, Scientific Results, 147, 255–291.

Gibbons, S. J. & Ringdal, F. (2006), The detection of low magnitude seismic events using array-based waveform correlation, *Geophysical Journal International*, 165, 149-166, doi: 10.1111/j.1365-246X.2006.02865.x

Gravemayer, I., Reston, T. J., & Moeller, S. (2013), Microseismicity of the Mid-Atlantic Ridge at 7ºS-8º15'S and at the Logatchev Massif oceanic core complex at 14º40'N-14º50'N. *Geochemistry Geophysics Geosystems*, 14, 3532-3554, doi: 10.1002/ggge.20197.

Harris, R. A. (1998), Introduction to special section: Stress triggers, stress shadows and implications for seismic hazard. *Journal of Geophysical Research*, 103, 24,347-24,358

Harmon, N., Rychert, C., Agius, M., Tharimena, S., Le Bas, T., Kendall, J. M. & Constable, S. (2018), Marine geophysical investigation of the Chain Fracture Zone in the equatorial Atlantic from the PI-LAB experiment. *Journal of Geophysical Research: Solid Earth*, 123, 11,016–11,030, doi:10.1029/2018JB015982

Harmon, N., Rychert, C. A., Kendall, J. M., Agius, M., Bogiatzis, P., & Tharimena, S. (2020), Evolution of the oceanic lithosphere in the equatorial Atlantic from Rayleigh wave tomography, evidence for small-scale convection from the PI-LAB experiment. *Geochemistry Geophysics Geosystems*, 21, e2020GC009174

Heaton, T. H. (1975), Tidal triggering of earthquakes. *Geophysical Journal International*, 43, 307-326

Heimann, S., Kriegerowski, M., Isken, M., Cesca, S., Daout, S., Grigoli, F., Juretze, C., Megies, T., Nooshiri, N., Steinberg, A., Sudhaus, H., Vasyura-Bathke, H., Willey, T., & Dahm, T. (2017), Pyrocko -an open-source seismology toolbox and library. GFZ Data Services, Potsdam, doi: 10.5880/GFZ.2.1.2017.001

Herrmann, M., & Marzocchi, W. (2020), Inconsistencies and lurking pitfalls in the magnitude–frequency distribution of high-resolution earthquake catalogs. *Seismological Research Letters*, 92, 909–922, doi: 10.1785/0220200337

Heimann, S., Isken, M., Kühn, D., Sudhaus, H., Steinberg, A., Vasyura-Bathke, H., Daout, S., Cesca, S., & Dahm, T. (2018). Grond - A probabilistic earthquake source inversion framework. V. 1.0. GFZ Data Services, Potsdam, doi: 10.5880/GFZ.2.1.2018.003 (https://doi.org/10.5880/GFZ.2.1.2018.003)

Hicks, S.P., Okuwaki, R., Steinberg, A., Rychert, C., Harmon, N., Abercrombie, R., Bogiatzis, P., Schlaphorst, D., Zahradnik, J., Kendall, J.M., Yagi, Y., Shimizu, K., & Sudhaus, H. (2020), Back-propagating supershear rupture in the 2016 Mw 7.1 Romanche transform fault earthquake. *Nature Geoscience*, 13, 647–653, doi: 10.1038/s41561-020-0619-9

Hilmo, R., & Wilcock, W. S. D. (2020), Physical sources of high-frequency seismic noise on Cascadia Initiative ocean bottom seismometers. *Geochemistry, Geophysics, Geosystems,* 21, e2020GC009085. https://doi.org/10.1029/2020GC009085

Horning, G., Sohn, R. A., Canales, J. P., & Dunn, R. A. (2018), Local seismicity of the Rainbow massif on the Mid-Atlantic Ridge, Journal *of Geophysical Research: Solid Earth*, 123, 1615–1630, doi: 10.1002/2017JB015288

Hofmann, A. W. (1997), Mantle geochemistry: the message from oceanic volcanism. *Nature*, 385, 219–229.

Hough, S. E., & Kanamori, H. (2002), Source properties of earthquakes near the Salton Sea triggered by the 16 October 1999 M 7.1 Hector Mine, California, Earthquake. *Bulletin of the Seismological Society of America*, 92(4), 1281–1289, doi: 10.1785/0120000910

Ide, S., Yabe, S., & Tanaka, Y. (2016), Earthquake potential revealed by tidal influence on earthquake size–frequency statistics. *Nature*, 9, 834-838, DOI: 10.1038/NGEO2796

Laske, G., Masters, G., Ma, Z., & Pasyanos, M. (2013), Update on CRUST1.0—a 1-degree global model of Earth's crust. *Geophysical Research Abstracts*, 15, 2658

Leptokaropoulos, K., Adamaki, A. A., Roberts, R. G., Gkarlaouni, C. G. & Paradisopoulou, P. M. (2018), Impact of magnitude uncertainties on seismic catalogue properties. *Geophysical Journal International*, 213, 940-951, https://doi.org/10.1093/gji/ggy023 (https://doi.org/10.1093/gji/ggy023).

Leptokaropoulos, K. (2020), Magnitude distribution complexity and variation at The Geysers geothermal field. *Geophysical Journal International*, 222, 893-906, doi: 10.1093/gji/ggaa208 (https://doi.org/10.1093/gji/ggaa208)

Leptokaropoulos, K. & Lasocki, S. (2020), SHAPE: A Matlab software package for time-dependent seismic hazard analysis. *Seismological Research Letters*, 91, 1867-1877, doi: 10.1785/0220190319 (https://doi.org/10.1785/0220190319)

Linker, J., & Dieterich, J. (1992), Effects of variable normal stress on rock friction: observations and constitutive equations. *Journal of Geophysical Research*, 97, 4923–4940, doi:10.1029/92JB00017

Lomax, A., Virieux, J., Volant, P., & Berge-Thierry, C. (2000), Probabilistic earthquake location in 3D and layered models. *Advances in Seismic Event Location*, 18, 101–134

Macdonald, K. C. (2001), Mid-ocean ridge tectonics, volcanism and geomorphology. *In: Encyclopedia of Ocean Sciences, Steele, J., Thorpe, S. and Turekian, K., eds., Academic Press*, 1798-1813

Marsaglia, G. & Marsaglia, J. (2004), Evaluating the Anderson-Darling distribution. *Journal of Statistical Software*, 9, 1-5

Mercier, H., & Morin, P. (1997), Hydrography of the Romanche and Chain Fracture Zones, *Journal of Geophysical Research*, 102(C5), 10, 373–10,389, doi: 10.1029/97JC00229

Mercier, H., & Speer, K. G. (1998), Transport of bottom water in the Romanche Fracture Zone and the Chain Fracture Zone. *Journal of Physical Oceanography*, 28(5), 779–790, doi: 10.1175/1520-0485(1998)028<0779:Tobwit>2.0.Co;2

Minson, S. E., Dreger, D. S., Bürgmann, R., Kanamori, H. & Larson, K. M. (2007), Seismically and geodetically determined nondouble-couple source mechanisms from the 2000 Miyakejima volcanic earthquake swarm. *Journal of Geophysical Research*, 112, B10308, doi:10.1029/2006JB004847

Parnell-Turner, R., Sohn, R.A., Peirce, C., Reston, T. J., Macleod, C. J., Searle, R. C., & Simão, N. M. (2017), Oceanic detachment faults generate compression in extension. *Geology*, v. 45, p. 923–926, doi: 0.1130/G39232.1

Parnell-Turner, R., Sohn, R.A., Peirce, C., Reston, T. J., Macleod, C. J., Searle, R. C., & Simão, N. M. (2020), Seismicity trends and detachment fault structure at 13ºN, Mid-Atlantic Ridge. *Geology*, v. 49, doi: 10.1130/G48420.1

Rice, J. R., & Cleary, M. P. (1976), Some basic stress diffusion solutions for fluid-saturated elastic porous media with compressible constituents. *Reviews of Geophysics*, 14, 227-24

Richter, C. F. (1958). *Elementary Seismology*, W. H. Freeman and Co., San Francisco, California, 578 pp

Rychert, C., Kendall, J. M., & Harmon, N. (2016), Passive Imaging of the Lithosphere-Asthenosphere Boundary [Data set]. *International Federation of Digital Seismograph Networks*, https://doi.org/10.7914/SN/XS_2016 (https://doi.org/10.7914

/SN/XS_2016)

Rychert, C. A., Harmon, N., Constable, S., & Wang, S. (2020), The nature of the lithosphere-asthenosphere boundary. *Journal of Geophysical Research: Solid Earth*, 125, e2018JB016463, doi: 10.1029/2018JB016463Rychert, C. A., Tharimena, S., Harmon, N., Wang, S., Constable, S., Kendall, J. M., Bogiatzis, P., Agius, M. R. & Schlaphorst, D. (2021), A dynamic lithosphere–asthenosphere boundary near the equatorial Mid-Atlantic Ridge. *Earth and Planetary Science Letters*, 566, 116949, https://doi.org/10.1016/j.epsl.2021.116949

Saikia, U., Rychert, C., Harmon, N., & Kendall, J. M. (2020), Sediment structure at the equatorial mid-atlantic ridge constrained by seafloor admittance using data from the PI-LAB experiment. *Marine Geophysical Research*, 41, 3, doi: 10.1007/s11001-020-09402-0

Saikia, U., Rychert, C., Harmon, N., & Kendall, J. M. (2021), Upper mantle anisotropic shear velocity structure at the equatorial Mid-Atlantic ridge constrained by Rayleigh wave group velocity analysis from the PI-LAB experiment. *Geochemistry Geophysics Geosystems*, 22, e2020GC009495, doi: 10.1029/2020GC009495

Scholz, C. H., Tan, Y. J., & Albino, F. (2019), The mechanism of tidal triggering of earthquakes at mid-ocean ridges. *Nature*, 10:2526, doi: 10.1038/s41467-019-10605-2

Schuster, A. (1897), On lunar and solar periodicities of earthquakes. *Proceedings of the Royal Society of London*, 61, 455–465

Simpson, R. W., & Reasenberg, P. A. (1994), *Earthquake-induced static stress changes on central California faults. In: The Loma Prieta, California Earthquake of October 17, 1989-Tectonic processes and models*, edited by R. W. Simpson U.S. Geol. Surv. Prof. Pap., 1550-F, F55-F89

Skempton, A. W. (1954), The pore-pressure coefficients A and B. Géotechnique, 4, 143-147

Stroup, D. F., Bohnenstiehl, D. R., Tolstoy, M., Waldhauser, F., & Weekly, R. T. (2007), Pulse of the seafloor: Tidal triggering of microearthquakes at 9 degrees 50'N East Pacific Rise. *Geophyical Research Letters*, 34, L15301, doi: 10.1029/2007gl030088 (https://doi.org/10.1029/2007gl030088)

Stroup, D. F., Tolstoy, M., Crone, T. J., Malinverno, A., Bohnenstiehl, D. R. & Waldhauser, F. (2009), Systematic along-axis tidal triggering of microearthquakes observed at 9o50’N East Pacific Rise. *Geophysical Research Letters*, 36, L18302, doi: 10.1029/2009GL039493

Sykes, L. R. (1970) Earthquake swarms and sea-floor spreading, *Journal of Geophysical Research*, 75, 6598-6611

Tan, Y. J., Tolstoy, M., Waldhauser, F., & Bohnenstiehl, D. R. (2018), Tidal triggering of microearthquakes over an eruption cycle at 9o50’N East Pacific Rise. *Geophysical Research Letters*, 45, 1825–1831, doi: 10.1002/2017GL076497

Tan, Y. J., Waldhauser, F., Tolstoy, M., & Wilcock, W. S. D. (2019), Axial Seamount: Periodic tidal loading reveals stress dependence of the earthquake size distribution (bvalue). *Earth and Planetary Science Letters*, 512, 39-45, doi: 10.1016/j.epsl.2019.01.047

Tanaka, S., Ohtake, M., & Sato, H. (2002), Evidence for tidal triggering of earthquakes as revealed from statistical analysis of global data. *Journal of Geophysical Research*, 107(B10), 2211, doi:10.1029/2001JB001577

Tesei, T., Harbord, C. W. A., De Paola, N., Collettini, C., & Viti, C. (2018), Friction of mineralogically controlled serpentinites and implications for fault weakness. *Journal of Geophysical Research: Solid Earth*, 123, 6976–6991, doi: 10.1029/2018JB016058

Teza, E., Scordilis, E. M. , Papazachos C. B. & Karakaisis G. F. (2016), An earthquake catalog of Mid-Atlantic Ridge, *Bulletin of the Geological Society of Greece*, vol. L, 1258-1269, doi: 10.12681/bgsg.11832 (https://doi.org/10.12681/bgsg.11832)

Tolstoy, M., Vernon, F. L., Orcutt, J. A., & Wyatt, F. K. (2002), Breathing of the seafloor: Tidal correlations of seismicity at Axial volcano. *Geology*, 30 (6), 503-506

Tsuruoka, H., Ohtake, M., & Sato, H. (1995), Statistical test of the tidal triggering of earthquakes: Contribution of the ocean tide loading effect. *Geophysical Journal International*, 122(1), 183–194

Utsu, T. (1999), Representation and analysis of the earthquake size distribution: a historical review and some new approaches. *Pure and Applied Geophysics*, 155, 509-535

van der Elst, N. J. (2021), B-positive: A robust estimator of aftershock magnitude distribution in transiently incomplete catalogs. *Journal of Geophysical Research: Solid Earth*, 126, e2020JB021027, doi: 10.1029/2020JB021027

Vuan, A., Sugan, M., Amati, G. & Kato, A. (2018), Improving the Detection of Low-Magnitude Seismicity Preceding the Mw 6.3 L'Aquila Earthquake: Development of a Scalable Code Based on the Cross Correlation of Template Earthquakes. *Bulletin of the Seismological Society of America*, 108, 471-480, doi: 10.1785/0120170106

Waldhauser, F., & Ellsworth, W. L. (2000), A double-difference earthquake location algorithm; method and application to the northern Hayward Fault, California. *Bulletin of the Seismological Society of America*, 90, 1353–1368, doi:10.1785/0120000006

Wang, S., Constable, S., Rychert, C. A., & N., Harmon (2020), A Lithosphere-Asthenosphere Boundary and Partial Melt Estimated Using Marine Magnetotelluric Data at the Central Middle Atlantic Ridge. *Geochemistry Geophysics Geosystems*, 21, e2020GC009177, doi: 10.1029/2020GC009177

Wilcock, W. S. D. (2001), Tidal triggering of micro earthquakes on the Juan de Fuca Ridge. *Geophysical Research Letters*, 28, 3999–4002

Wilcock, W. S. D. (2009), Tidal triggering of earthquakes in the Northeast Pacific Ocean, *Geophysical Journal International*, 179, 1055-1070, doi: 10.1111/j.1365-246X.2009.04319.x

Wilcock, W. S. D., Tolstoy, M., Waldhauser, F., Garcia, C., Tan, Y. J., Bohnenstiehl, D. R., Caplan-Auerbach, J., Dziak, R. P., Arnulf, A. F., & Mann, M. E. (2016), Seismic constraints on caldera dynamics from the 2015 Axial Seamount eruption. *Science*, 354, 1395–1399